

# A statistical method for inferring the Initial Mass Function of young clusters I: Procedure

Babar Ali

*Infrared Processing and Analysis Center, MC 100-22  
California Institute of Technology, Pasadena, CA 91125*

`babar@ipac.caltech.edu`

## ABSTRACT

I present a new method for inferring the Initial Mass Function (IMF) of young clusters based on intrinsic  $K$ -band Luminosity functions (LFs). This technique uses a diagnostic based on number-ratios (NRs) of stars in three 1-mag wide luminosity bins centered at absolute  $K$ -band magnitudes of 1.5, 3 and 5 mag. Two NRs are calculated:  $R_1$ , based on the two high luminosity bins, and  $R_2$ , based on the two low luminosity bins. Synthetic LFs (for a given IMF and a range of coeval and non-coeval cluster populations) are used to estimate the effects of both the underlying IMF and the ages of cluster members on these NRs.

X  
(e)  
I find that (i) for a given IMF, the range of values for  $R_1$  and  $R_2$  are well constrained for both coeval and non-coeval cluster ages. (ii) Changing the underlying IMF changes the mean values of the  $R_1$  and  $R_2$  distribution resulting in an “offset”. (iii) This “offset” is correlated with the “direction” (*i.e.* ratio of high- to low-mass stars) in which the IMF is changed. These results suggest that a statistical goodness-of-fit test (*e.g.* the two-dimensional Kolmogorov-Smirnoff test) can be used to compare an ensemble of observationally derived intrinsic cluster LFs and the synthetic LFs. Since both the adopted IMF and star-formation histories of the synthetic LFs are known, this comparison allows one to reject or accept the following two hypotheses with statistical confidence: (a) is the IMF of present-day clusters consistent with the solar-neighbour IMF, and, more generally, (b) is a single IMF consistent with the observed sample of clusters. For a suitably chosen set of clusters, the latter has strong constraints for the extent to which environmental differences in the parent cloud can alter the form of the IMF. Finally, observational considerations are presented for carrying out this experiment.

## 1. Introduction

The census of star-formation provided by optical and infrared imaging surveys has shown that star-formation occurs within molecular clouds in groups or clusters, sometimes with hundreds of stars (for a review, see Meyer *et al.* 2000). Most of the cluster population is deeply embedded within the dust enshrouded cloud cores and is invisible at optical wavelengths. The Initial Mass Function (IMF; the number distribution of stars per mass) of these groups and clusters is the end product of the star-formation process. The form of the IMF depends largely on the physics of molecular cloud fragmentation and the subsequent history of the stellar populations formed. Thus, an understanding of the IMF and of the factors which affect its origin is of fundamental importance to the development of a theory of star formation (*e.g.* Adams & Fatuzzo 1996), and subsequent galactic evolution and chemical enrichment (Miller & Scalo 1979).

The IMF of stars in young clusters is observationally difficult to obtain since stellar masses are difficult to measure directly; Only preliminary data on pre-main sequence (PMS) binary systems is currently available. Thus, star formation researchers have traditionally used cluster luminosity functions (LFs; the observed number distribution of stars per broadband magnitude) to infer the underlying IMF of young stars. LFs are advantageous in that they provide photometry information for all cluster members to faint flux (and presumably mass) limits. However, since the observed luminosities of young stars depend upon both the underlying mass and the age of star, direct conversion of the cluster LF to an IMF requires additional knowledge about the ages of the cluster members. Zinnecker *et al.* (1993), Ali *et al.* (1995), Lada & Lada (1995), and others, have shown that the, generally unknown, evolutionary status of young stars significantly alter the observed form of the LFs and, hence, severely limit the usefulness of LFs in inferring the underlying IMF. Recently, Muench *et al.* (2000) extended the earlier modeling efforts by using monte-carlo simulations of young clusters rather than the analytical forms followed by the previous authors. Muench *et al.* (2000), however, only considered a single star-formation history: randomly formed stars within an adopted age spread. Systematic star-formation scenarios, *e.g.* trends with mass, *etc.*, or multiple epochs of star-formation in the same cluster are not considered.

Alternatively, spectroscopic analysis has been used to place cluster members on the H-R diagram. The mass and age information for each star is then inferred independently by comparing H-R diagram location with predictions from pre-main sequence (PMS) evolutionary models. Hillenbrand (1997) used optical spectroscopy to construct an H-R diagram for 979 stars in the Orion star-forming region. Ali (1996), Meyer (1996), and Luhman (1999), among others, have made similar attempts using near-infrared spectroscopy to study the embedded, optically invisible population of young clusters. spectroscopic analysis remains the

most reliable option for determining the IMF until direct mass determination for statistically large samples of cluster members are available. However, these time-consuming studies are generally limited to the small, brighter or optically visible, subsamples of the total cluster populations with statistically significant sample available only for the Orion nebula cluster (Hillenbrand 1997).

Given the above difficulties in determining the IMF of young, dust-embedded clusters, these studies have only just begun to address the following two (related) fundamental questions: (1) Is the IMF of stars in currently active star-formation regions similar to that of the solar neighborhood? And, more generally, (2) is a single IMF (of any form) consistent with all present-day cluster populations? For suitably selected Galactic clusters, the answer to the second question will strongly constrain the extent to which environmental differences in star-forming regions affect the form of the IMF. Obtaining answers to both questions is further made difficult by the observed complexities in the LFs; Both the observed and synthetic LFs of young clusters are not adequately characterized by simple analytical fits (*e.g.* power-laws) which makes quantitative comparisons difficult.

In this contribution, I describe a methodology for comparing an ensemble of observed clusters with an ensemble of synthetic clusters using statistical goodness-of-fit tests for the comparison. Because both the ages and the IMF of stars in the synthetically constructed clusters are known, one can accept or reject consistency between observations and the models with statistical confidence. When the synthetic clusters are constructed using the solar-neighborhood IMF, this comparison can address question (1) posed above. Further, by using IMFs with various forms and complexity the comparison can address question (2) also posed above.

This procedure uses photometry to ensure statistically complete sampling of the cluster population. The *K*-band is best suited for these photometry surveys. At wavelengths shorter than  $2.2\mu\text{m}$  extinction effects become important for the obscured cluster population. At longer wavelengths, the observed flux from PMS stars is frequently contaminated by emission from their circumstellar (and generally spatially unresolved) environment. Further, large-format imaging arrays with low characteristic noise levels are readily available for near-IR surveys.

The organization of the paper is as follows: Section 2 describes the proposed *K*-band number ratio diagnostic. Section 3 describes the modeling effort. Section 4 describes and discusses the results and procedure. Finally, observational considerations for constructing the proper *K*-band LFs are described in Section 5.

## 2. The number ratio diagnostic

The  $K$ -band LFs are characterized with number ratios of stars in three luminosity bins with centers at  $M_K=1.5$ , 3, and 5 mag. The bins are 1 mag wide to accommodate the expected observational errors (Section 5). Figure 1 illustrates these definitions on the LFs for a 1 Myr old cluster (see Section 3 for details on the construction of the KLF). The diagnostic bands with centers at  $M_K=1.5$ , 3, and 5 mag are labelled as  $N_1$ ,  $N_2$ , and  $N_3$ , respectively, on Figure 1. The two number ratios, thus obtained, are:

$$R_1 = \frac{N(1.5)}{N(3)}, \text{ and } R_2 = \frac{N(5)}{N(3)};$$

where,  $N(M_K)$  is the number of stars in bin with center at  $M_K$ .

The ratios  $R_1$  and  $R_2$  are chosen to provide sensitivity to higher and lower luminosity stars, respectively. These ratio are sensitive to stars with masses in the range  $0.08 M_\odot \leq M \leq 2.5 M_\odot$  (*i.e.* T Tauri stars). Fluxes of higher mass (Herbig Ae/Be) stars are additionally complicated by their strong interaction with the parent cloud and are, hence, not considered in this analysis.

## 3. Synthetic LF Modeling

The synthetic LFs are constructed to explore the effects of stellar evolution and the underlying IMF on the two number ratios, and to characterize their usefulness in decoupling mass and age information for the clusters. These results are needed to provide the basis from which to reject or accept the hypothesis that an observed distribution of clusters is consistent with a given IMF. This point is discussed further in Section 4. We discuss the methodology here.

The procedure used here for constructing LFs is semi-analytical and similar to the one described by Zinnecker *et al.* (1993), Ali *et al.* (1995), and Lada & Lada (1995). The number of stars in a given luminosity bin whose edges are defined by  $K$ -band magnitudes,  $K_1$ , and  $K_2$  is:

$$\begin{aligned} \text{KLF}(K_1 < K \leq K_2) &= \int_{K_1}^{K_2} \frac{dN}{dK} dK \quad \text{and,} \\ \frac{dN}{dK} &= \frac{dN}{d \text{Log}_{10} \text{Mass}} \times \frac{d \text{Log}_{10}(\text{Mass})}{dK} \end{aligned} \quad (1)$$

where,  $N$  is the number of stars,  $K$  is the observed  $K$ -band magnitudes, and 'Mass' refers to the masses of stars. Thus,  $\frac{dN}{d \text{Log}_{10}\text{Mass}}$  is the IMF and  $\frac{d \text{Log}_{10}(\text{Mass})}{dK}$  provides the conversion from mass to observed magnitudes. The integral is needed to obtain the total number of stars in a given luminosity bin. The process is repeated for each luminosity bin of interest.

The relationships listed above identify the main ingredients for constructing the synthetic LFs: The IMF, and the pre-main sequence mass-to- $K$  magnitude relation. The former is adopted, and the latter depends on the star-formation history of the cluster, and theoretical calculations for the pre-main sequence evolution of stars. Additionally, the theoretical studies typically provide bolometric luminosities which must be converted to observable  $K$ -band magnitudes by using suitable bolometric corrections. Each of these ingredients is further discussed below.

### 3.1. The IMF

Three types of IMFs are considered: (i) The averaged solar neighbourhood IMF given by Miller & Scalo (1979) (hereafter referred to as MS79), (ii) power-law IMFs, given by:

$$\frac{dN}{d \text{Log}_{10}\text{Mass}} \propto M^\gamma$$

Where  $M$  is the mass of the star and  $\gamma$  is the power-law index, and (iii) half-normal IMFs similar to the MS79 IMF but chosen to deliberately alter the ratio of high- to low-mass stars, compared to the MS79 IMF. These IMFs are selected to provide a plausible range of IMFs in order to investigate and characterize the effects of the underlying IMF on the observed  $K$ -band LFs. These IMFs are used for illustrative purposes in this study. I have also assumed that clusters form a complete IMF during star-formation process. Truncated or incomplete IMFs are not considered.

### 3.2. The star-formation history

Besides the IMF, the star-formation history most critically determines the form of an observed LF (see *e.g.* Ali & DePoy 1995). To provide an effective basis for comparison, the synthetic LFs must be constructed from all plausible star-formation scenarios so that evolutionary effects are fully considered.

The simplest scenario is that of a single burst in which all stars form (or first appear as

stars) simultaneously. The observed ages of stars in the Orion (Hillenbrand 1997) and Taurus (Luhman 1999), however, suggest that such simple scenario is unlikely to be realistic. Hillenbrand (1997) observe both a significant range of ages and a systematic trend in ages of the Orion nebula cluster members. Luhman (1999) observe a range of ages for Taurus. While systematic effects in the PMS evolutionary models may be responsible for these effect (Hillenbrand 1997), non-coeval history of clusters cannot be ruled out.

Clusters can form non-coeval populations in one of the three ways: (i) multiple complete bursts. In this case, the cloud undergoes two or more epochs of forming young stars. (ii) Stars may form with systematic trends in the ages with mass. For example, low-mass stars form first. And, (iii) the star-formation process produces stars at random *i.e.* uniform distribution of ages.

Various theoretical considerations can be made for the origin of age spreads in young clusters (see *e.g.* Adams & Fatuzzo 1996, Clarke *et al.* 2000, and Elmegreen *et al.* 2000 ). However, for the purpose of this study, the detailed form of the cluster age spread that is used to construct the LFs is motivated by only one factor: a suitable sampling of plausible star-formation histories to provide an effective basis for comparison. In this respect, the conservative approach is to include as many stellar birth history scenarios as possible, including some that may appear unlikely. The only disadvantage of including these is a possible broadening of the range of values for the two number ratios  $R_1$  and  $R_2$ . This is further discussed in Section 4.

Under these considerations listed above, four star-formation scenarios are considered:

**Single ages**(hereafter referred to as **ISO**). Clusters with ages at 0.1, 0.5, 1, 2, 3, 5, 10, and 100 Myr are considered. These ages correspond to those typically observed for the youngest star-forming regions. Further, it is assumed that while the ages are sampled at the discrete points listed above, the underlying changes on the number ratios are smooth.

**Multiple bursts**(hereafter referred to as **SUM**). Multiple complete bursts are obtained by combining data from the single age clusters. In doing so, all possible combinations for the single age clusters (listed above) are considered.

**Systematic age trends**. I considered two forms of systematic age trends: linear (**LIN**) and exponential (**EXP**). That is the difference in the age between successive masses is linear or exponential. These two form the “extremes” for such systematic trends in ages. Further, within each of the above two schemes the trend can either be from low- to high-mass stars or from high- to low- mass stars. For the latter case, the linear and exponential scenarios are referred to as **LIR** and **EXR**, respectively.

**Random**(hereafter referred to as **RAN**). In this scenario, stars form at random times during the period of star-formation, resulting in a uniform distribution of ages by mass. As for the SUM scenario, the age spreads for all possible combinations of single age cluster values (listed above) are considered.

### 3.3. The PMS Mass–Magnitude relation

The PMS evolutionary models are needed to obtain the Mass–Magnitude relationship. The PMS model used in this study are from D’Antona & Mazzitelli (1997). In addition D’Antona & Mazzitelli (1994), Baraffe *et al.* (1998), Siess *et al.* (2000), and Palla & Stahler (1993) provide PMS evolutionary models. While considerable differences exist between the the adopted numerical methods, input physics and theoretical assumptions, Muench *et al.* (2000) find that varying the underlying PMS evolutionary models has little effect on computed KLFs.

A more significant consideration of the PMS evolutionary tracks is the coverage in mass. The mass range considered here is not provided by any one set of tracks, and it was necessary to splice results from two different tracks to form a complete coverage. I used the D’Antona & Mazzitelli (1994) and (1997) models for this purpose. This procedure is described in more detail in Appendix A.

### 3.4. *K*-band bolometric corrections

D’Antona & Mazzitelli (1994) and (1997) provide bolometric luminosities which must be converted to the *K*-band magnitudes for the purpose of this study. This correction is calculated by assembling and calculating effective temperature and bolometric corrections from several authors. This procedure is described in Appendix B. The bolometric *K*-band correction is estimated from this assembly as the average value of all sources at that effective temperature. This standard deviation of such values is, on average, 0.07 mag. The number ratios thus calculated are not effected since these are derived from 1 magnitude wide bins.

## 4. Results and discussion

Figure 2 shows the results from the synthetic KLFs on a plot of  $R_2$  vs.  $R_1$  using the field stars IMF, MS79. The star-formation histories are also individually identified using labels from Section 3. The solid line shows the progression of a single age cluster from 0.1 Myr to

100 Myr. Non-coeval clusters duplicate the trend shown by single age clusters but further broaden the range of values of single age clusters.

For a given IMF and coeval clusters, the ratio  $R_1$  has the highest value when stars are at their youngest ages (more high luminosity stars). The value of  $R_1$  successively decreases as the cluster ages and the stars migrate towards lower luminosity bins. Similarly, the value of  $R_2$  increases as the clusters become older. The change in  $R_2$  vs.  $R_1$  is, however, not linear. These trends are similar but less well-defined for non-coeval clusters.

Figures 3 & 4 illustrate the effect of changing the underlying IMF on the number ratios. Figure 3 shows the IMF used. The MS79 IMF is also shown (as dotted line) for comparison. Figure 4 shows the resulting number-ratio values in corresponding panels. The IMFs are chosen such that the number of stars produced by the IMF in either the region  $0.1 \leq M/M_\odot \leq 1$ , or the region  $1 \leq M/M_\odot \leq 2.5$  is significantly different from the MS79 IMF.

There are three significant results from this exercise:

1. The range of values of  $R_1$  and  $R_2$  is well constrained for a given IMF for all birth-rate histories considered (Figure 4).
2. Although the resulting number ratios partially overlap the region occupied by the MS79 IMF, there is a significant “shift” in the pattern of values for the number ratios when the underlying IMF is changed (Figure 4).
3. The “shift” is correlated with the *direction* in which the underlying IMF is changed. By increasing the the low-mass content, one finds decreased  $R_1$  values and increased values for  $R_2$ . Contrarily, increasing the high-mass content of the IMF significantly decreases the values for  $R_2$ .

These results suggest that *by using a suitable two-dimensional goodness-of-fit test, a statistical comparison is possible between an observed set of clusters and the synthetic LFs.* The most suitable statistic is the two-dimensional Kolmogorov-Smirnoff (2DKS) test. This test is described by Fasano & Franceschini (1987). For an example of its use see Metchev & Grindlay (2002). The 2DKS test is particularly well-suited for low-number statistics which are expected for this study, and is, thus, preferred over similar but less efficient two-dimensional  $\chi^2$  test.

Since the IMF and the ages of clusters used to construct the synthetic LFs are known, the statistical test can then be used to address the two fundamental questions posed in Section 1: (1) Is the IMF of the observed clusters consistent with MS79 IMF? That is, are the observed values of  $R_1$  and  $R_2$  consistent with those obtained by using the MS79

IMF? And, more generally, (2) is there a single IMF that is consistent with the observed distribution of clusters? Further, if the sample of observed clusters is chosen to span a range of observed cluster formation environments, then point (2) above also constrains the extent to which these environmental differences alter the form of the IMF.

The 2DKS allows both hypothesis (listed above) to be rejected or accepted with statistical confidence in comparison with the values from the synthetic LFs. The answer to the first question is obtained by computing a 1-sample 2DKS statistic. The answer to the second question is more complicated. It isn't possible to "reverse engineer" a best-fit IMF since even when the IMF are simple analytical functions, the star-formation history may not necessarily be. Instead, the 1-sample 2DKS statistic must be obtained for each adopted IMF until one can be accepted. The form of the IMF itself can be varied to more complicated forms if simple descriptions are insufficient. For example, the IMF can be evolved to multi-segmented power-laws if single index power-law IMFs are insufficient. The strength of this procedure is in addressing the relevant questions via the statistical comparison, rather than trying to infer a direct form of the IMF for each individual cluster.

## 5. Observational considerations

As stated in Section 1, intrinsic  $K$ -band LFs are best-suited for this experiment. These KLFs must be photometrically complete. The photometry completion limit is derived by adding extinction and the distance modulus to the faint edge of the lowest luminosity bin ( $M_K=5.5$  mag). For the Orion star-forming region, this translates to a limiting  $K$ -band magnitude of about 18.5 mag, assuming a distance modulus of 8.0 mag and the expected maximum extinction of 5 mag at  $K$  (an insignificant number of stars will have extinction values beyond this limit).

The observed KLFs must also be corrected for extinction and excess emission effects to obtain the intrinsic KLFs needed for this study. The term excess emission is used here to refer to any emission above the photospheric emission of the star that cannot be resolved or accounted for in the photometry measurement. This is generally thought to arise in circumstellar material, though the details (*e.g.* geometry) are less well understood.

The corrections for both the extinction and the excess emission is obtained from the location of the stars on near-IR color-color plot. This requires that photometry for all sources is available in all photometric bands, and that the observer has *a priori* knowledge of the intrinsic colors of the star. One can assume that all stars have the intrinsic colors of a K5 V star. And that the excess emission is given by an averaged excess vector on a color-color

plot (Meyer 1996). Given the  $\sim \pm 0.3$  mag differences in the intrinsic near-infrared colours of stars and the scatter about the averaged excess vector, the observed number counts will be accurate in the adopted 1 mag wide bins under these assumptions.

Additionally, there are two statistical corrections to the observed number of stars in a given luminosity bin. One is for the expected but undetected secondary stars which are companions to higher luminosity stars. The other is for field star contamination. The latter is easily corrected by incorporating nearby fields to estimate the non-cluster population. The former is more complex, but since only a statistical correction (*e.g.* such as the one given by Palla & Stahler 1993) is required, detailed knowledge about the PMS binarity for each cluster is not necessary.

## 6. Summary

This work is aimed at answering the following two questions. (1) is the IMF of young clusters consistent with that obtained from the solar-neighborhood? And, particularly, (2) is a single IMF consistent with all present day clusters?

A number-ratio diagnostic (Section 2, Figure 4) is devised to address these questions. The effects of the IMF and stellar evolution on the number ratios are explored by constructing synthetic LFs (Section 3). The results from the synthetic LFs (Section 4) suggest that (i) the number-ratios are well-constrained for a given IMF, even when a range of birth-rate histories are considered. (ii) There is an offset in the values of the number-ratios as the underlying IMF is varied, and (iii) the direction of this offset is correlated with the direction in which the IMF is varied.

Since the values of the number-ratios are well-constrained for a given IMF, the observed LFs can be statistically compared with those derived using synthetic LFs. Thus, the two hypothesis listed above can be accepted or rejected with statistical confidence.

The author wishes to thank Barry Madore for useful discussions on the use of statistics for analysis

### A. Splicing PMS tracks for complete mass coverage

The pre-main sequence tracks from D'Antona & Mazzitelli (1997) are used to prepare the synthetic LFs. These authors only provide information for stars up to  $1.5 M_{\odot}$ . Higher

mass T-Tauri stars, up to  $2.5 M_{\odot}$ , are supplemented from the authors earlier work (D’Antona & Mazzitelli 1994). Only the ratio  $R_1$  is affected by the “missing” higher masses, and that only for those bins which contain the higher mass stars. Empirical investigations show that while there is no simple relationship between  $R_1$  values derived using the tracks from D’Antona & Mazzitelli (1994) and those from D’Antona & Mazzitelli (1997), one finds that

$$R_1(1997) = R_1(1994) + C0 + C1 * R_2(1997)$$

The values for the constants C0 and C1 is derived from the set of values for which both  $R_1$  values exist. For this subset, comparing values of  $R_1$  derived in this manner with actual  $R_1$  values shows a standard deviation of 0.08 in the derived value of  $R_1$ .

### B. K-band bolometric corrections

The K-band bolometric corrections are either adopted or calculated from the following sources:

Alonso *et al.* (1996): K-band bolometric corrections are provided.

Bessell (1998): K-band bolometric corrections are provided using theoretical model atmospheres.

Houdashelt *et al.* (2000): K-band bolometric corrections are provided.

Kenyon & Hartmann (1995): K-band bolometric corrections are calculated from the bolometric correction at V and the V-K color.

Lejuene (1998): Bolometric correction at K are calculated from the bolometric correction at V, and the V-K color.

Pickles (1998): K-band bolometric corrections are provided

### REFERENCES

- Adams, F. C., Fatuzzo, M. 1996, ApJ, 464, 256  
 Ali, B. 1996, Ph.D. Thesis, The Ohio State University  
 Ali, B., & DePoy, D. L. 1995, AJ, 109, 709

- Alonso, A., Arribas, S., & Martinez-Roger, C. 1996, *A&AS*, 313, 873
- Baraffe, I., Chabrier, G., Allard, F., & Hauschildt, P. H. 1998, *A&A*, 337, 403
- Bessell, M. S., Castelli, F., & Plez, B. 1998, *ã*, 333, 231
- Clarke, C. J., BOnnell, I. A., & Hillenbrand, L. A. 2000 in *Protostars and Planets IV*, eds. V. Mannings, A. P. Boss, & S. S. Russell (Tucson: Univ. of Arizona Press), 151
- D'Antona, F., & Mazzitelli, I. 1994, *ApJS*, 41, 467
- D'Antona, F., & Mazzitelli, I. 1997, in *Cool Stars in Clusters and Associations*, eds. G. Micela & R. Pallavicini, *Mem. S. A. It.*, 68, 807
- Elmegreen, B. G., Efremov, Y., Pudritz, R. E. & Zinnecker, H. 2000, in *Protostars and Planets IV*, eds. V. Mannings, A. P. Boss, & S. S. Russell (Tucson: Univ. of Arizona Press), 179
- Fasano, G. & Franceschini, A. 1987, *MNRAS*, 225, 155
- Hillenbrand, L. A. 1997, *AJ*, 114, 198
- Houdashelt, M. L., Bell, R. A., Swigart, A. V., & Wing, R. F. 2000, *AJ*, 119, 1424
- Kenyon, S. J., & Hartmann, L. W. 1995, *ApJS*, 101, 117
- Lada, E. A., & Lada, C. J. 1995, *AJ*, 109, 1682
- Lejeune, T., Cuisinier, F., & Buser, R. 1998, *A&AS*, 130, 65
- Luhman, K. L. 1999, *ApJ*, 525, 466
- Metchev, S. A., Grindlay, J. E. 2002, *MNRAS*, 335, 73
- Meyer, M. 1996, Ph.D Thesis, University of Massachusetts
- Meyer, M., Adams, F. C., Hillenbrand, L. A., Carpenter, J. M., & Larson, R. B. 2000 in *Protostars and Planets IV*, eds. V. Mannings, A. P. Boss, & S. S. Russell (Tucson: Univ. of Arizona Press), 121
- Miller, G. E., & Scalo, J. M. 1979, *ApJS*, 41, 513
- Muench, A. A., Lada, E. A., & Lada, C. J. 2000, *ApJ*, 533
- Pickles, A. J. 1998, *PASP*, 110, 863

Palla, F., & Stahler, S. W. 1993, ApJ, 418, 414

Siess, L., Dufour E., & Forestini, M. 2000, *â*, 358, 593

Zinnecker, H., McCaughrean, M., & Wilkings, B. A. 1993, in Protostars and Planets III, eds. H. Levy and J. I. Lunine (Tucson: Univ. of Arizona Press), 429

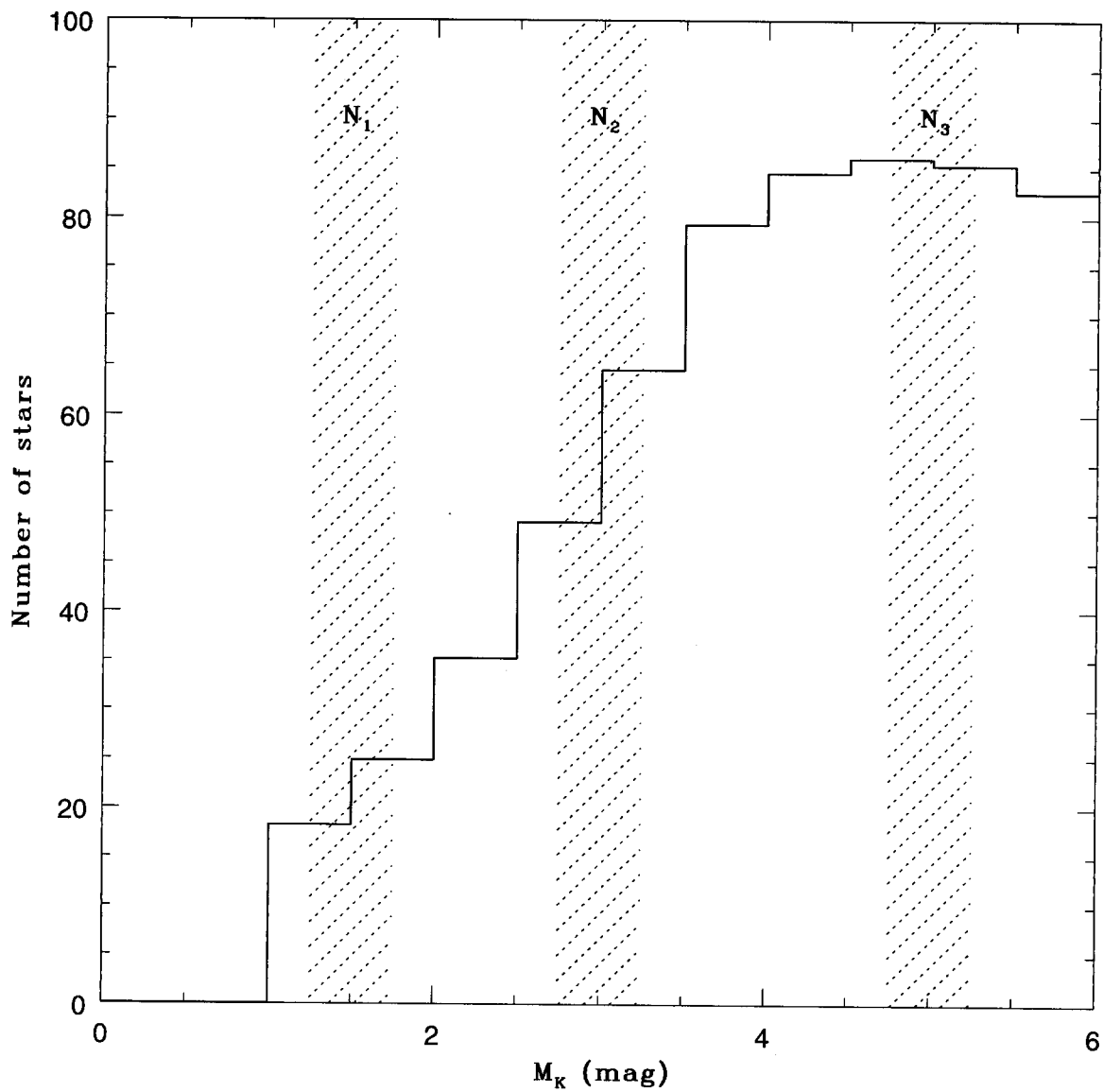


Fig. 1.— The definition of the three luminosity bins used for the number ratio diagnostic. The histograms show the simulated LFs of a 1 Myr old co-eval cluster. The shaded regions show the three bins used for this study.

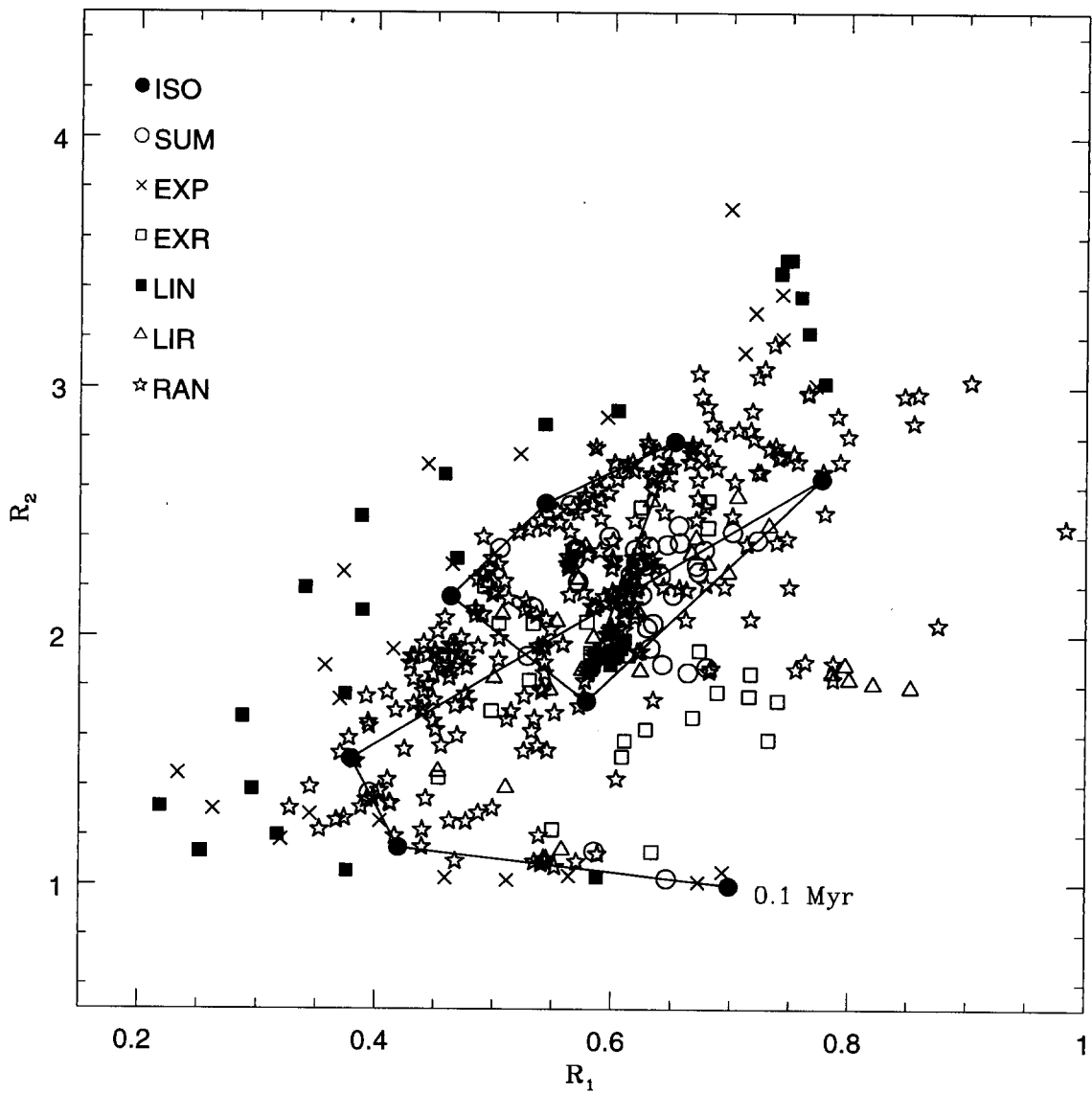


Fig. 2.— The number-ratio diagnostic for the MS79 IMF. The different symbols show results from the star-formation histories considered here. Each is identified in the upper-left hand corner (see text for label definitions). The solid line connects the value for the single age clusters. The youngest age considered here is also identified as the “starting point”.

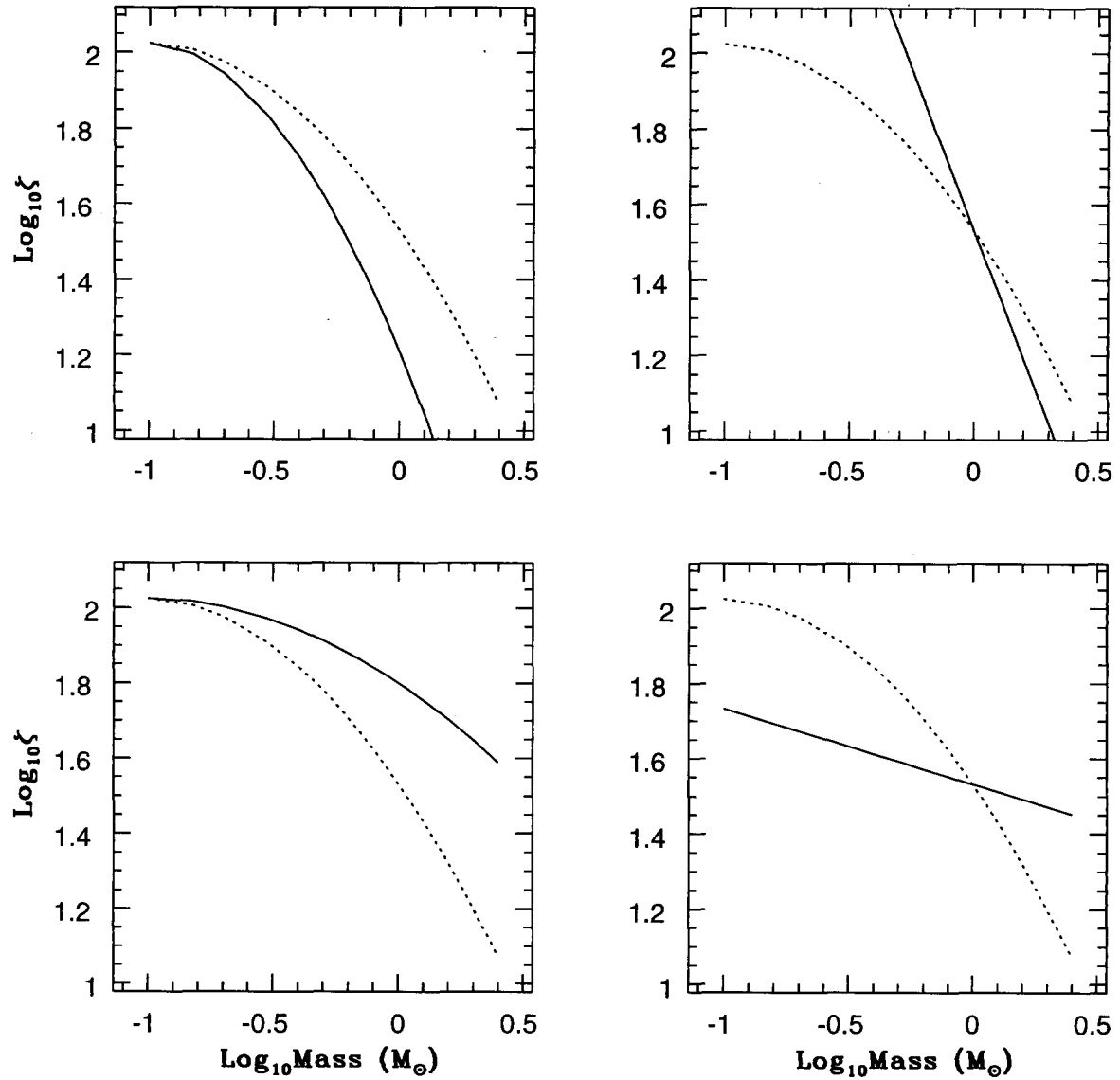


Fig. 3.— The additional IMFs used to construct the synthetic LFs. For comparison the MS79 IMF is shown as dotted line in each panel. The two panels on the left show half-normal IMFs. The two right-hand panels show power-law IMFs. The steepest power-law IMF, upper right panel, is only partially shown to keep axis values similar in all panels and to clearly show the differences.

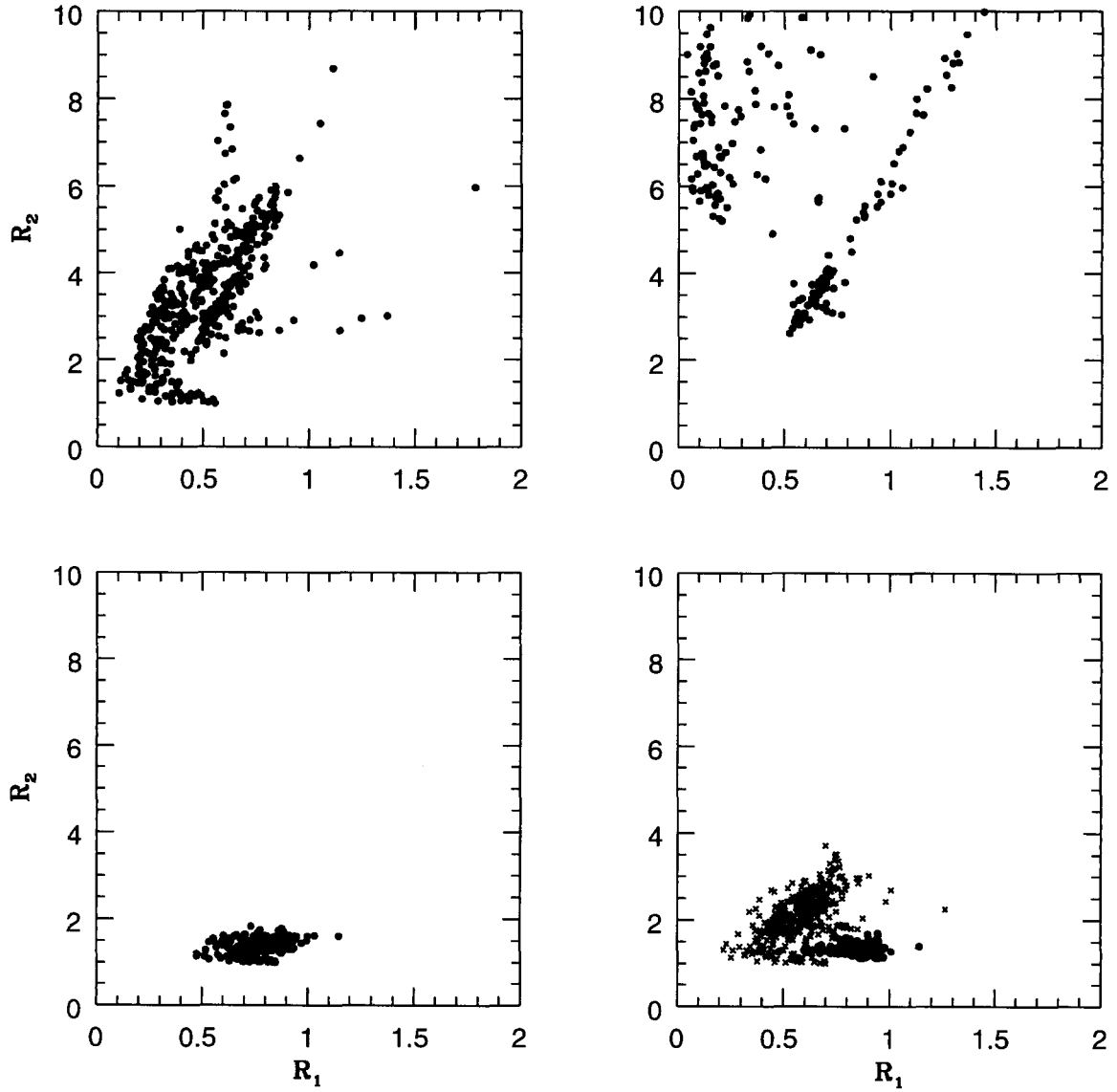


Fig. 4.— The number-ratios resulting from the four IMFs from Figure 3. The panel placement is the same. For comparison, the MS79 number-ratio values are also shown in the bottom right panel as open circles. As for Figure 3 the results from the steepest power-law are only partially shown.